Infection and Drug Resistance

Dovepress
Taylor & Francis Group

Open Access Full Text Article

ORIGINAL RESEARCH

Serum Exosomes miR-122-5P Induces Hepatic and Renal Injury in Septic Rats by Regulating TAK1/SIRT1 Pathway

Jiaqi Wang, Yujing Jiang, Yamin Yuan, Xin Ma, Tongqin Li, YaTing Lv, Jing Zhang, Liao Chen, Jinquan Zhou, Yanfei Meng, Bei Zhang, Xiaorong Dong, Li Ma

Department of Critical Care Medicine, Lanzhou University Second Hospital, Lanzhou University, Lanzhou City, Gansu Province, People's Republic of China

Correspondence: Li Ma, Email ery_mali@lzu.edu.cn

Aim: Sepsis is a potentially fatal condition characterized by organ failure resulting from an abnormal host response to infection, often leading to liver and kidney damage. Timely recognition and intervention of these dysfunctions have the potential to significantly reduce sepsis mortality rates. Recent studies have emphasized the critical role of serum exosomes and their miRNA content in mediating sepsis-induced organ dysfunction. The objective of this study is to elucidate the mechanism underlying the impact of miR-122-5p on sepsis-associated liver and kidney injury using inhibitors for miR-122-5p as well as GW4869, an inhibitor targeting exosome release.

Materials and Methods: Exosomes were isolated from serum samples of septic rats, sepsis patients, and control groups, while liver and kidney tissues were collected for subsequent analysis. The levels of miR-122-5p, inflammation indices, and organ damage were assessed using PCR, ELISA, and pathological identification techniques. Immunohistochemistry and Western blotting methods were employed to investigate the activation of inflammatory pathways. Furthermore, big data analysis was utilized to screen potential targets of miR-122-5p in vivo.

Key Findings: Serum exosomal levels of miR-122-5p were significantly elevated in septic patients as well as in LPS-induced septic rats. Inhibition of miR-122-5p reduced serum pro-inflammatory factors and ameliorated liver and kidney damage in septic rats. Mechanistically, miR-122-5p upregulated TAK1, downregulated SIRT1, and facilitated NF-κB activation.

Conclusion: Serum exosomal miR-122-5p promotes inflammation and induces liver/kidney injury in LPS-induced septic rats by modulating the TAK1/SIRT1/NF-κB pathway, highlighting potential therapeutic targets for sepsis management.

Keywords: sepsis, exosome, miR-122-5p, NF-κB signaling pathway, sepsis-related liver and kidney injury

Introduction

Sepsis has emerged as a prominent global cause of mortality, with an estimated annual incidence of approximately 11 million sepsis-related deaths, accounting for 19.7% of all global fatalities.[1] Currently, the management of sepsis encompasses fluid resuscitation, infection control, and tissue perfusion maintenance as part of a comprehensive therapeutic approach; however, there has been limited reduction in mortality rates. The pathogenesis of sepsis involves the accumulation of diverse pro-inflammatory factors during the course of inflammatory response and immune dysfunction.[2] The inflammatory cascade during sepsis is a critical event, with NF-κB serving as the pivotal mediator. The activation of NF-κB is regulated by upstream signaling molecules, including TGF-activated Kinase 1 (TAK1) and silencing regulatory protein 1 (Sirtuin 1).

Exosomes are derived from multivesicular bodies (MVBs), a type of extracellular vesicles (EVs). Under an electron microscope, exosomes exhibit a cup-like morphology and are naturally released by various types of living cells, including macrophages, mesenchymal stem cells, epithelial cells, and dendritic cells. These exosomes can be detected in different bodily fluids such as blood, saliva,[3] urine, ascites, semen, broncho-alveolar lavage fluid, breast milk,[4] airway

Received: 22 October 2024
Accepted: 1 January 2025
Published: 9 January 2025

secretions,[5] and cerebral spinal fluid.[6–8] Their diverse contents encompass nucleic acids, proteins, lipids, amino acids, and metabolites, thereby serving as indicative markers of the parental cell's physiological state.[9] Moreover, exosomes possess remarkable stability that prevents them from rupturing, allowing them to travel long distances in the bloodstream and evade proteolysis and phagocytosis. This characteristic suggests that exosomes hold potential value for diagnosis and treatment (as drug delivery vehicles) of clinical diseases.[10] The functional roles of exosomes have been studied in various diseases, such as inflammation,[11,12] cancer,[13] diabetes,[14] and renal disorders.[15] Circulating exosomes have been linked to cytokine storm, complement and coagulation cascades,[16,17] the endothelium barrier, protein degradation, and vitamin metabolism in sepsis patients.[18]

The effects of exosomes on immune cells are predominantly mediated by non-coding RNAs, including microRNAs (miRNAs), long non-coding RNAs (lncRNAs), and circular RNAs (circRNAs). Among these non-coding RNAs, miRNA is the most abundant in exosomes. MiRNAs are approximately 21 nucleotides in length and play crucial roles in the cellular metabolism of eukaryotic organisms. Moreover, miRNA exhibits remarkable stability in body fluids due to its resistance to degradation by RNA enzymes.[19,20] Additionally, miRNAs are highly conserved across species and have been implicated in numerous diseases.[21–23] It has been confirmed that miRNAs possess the capability to regulate the transcription and translation of inflammatory genes during the induction of LPS tolerance.[24] Additionally, the exosomal miRNAs and mRNAs from patients with septic shock related to pathogenic pathways like inflammation, oxidative stress, and cell cycle control.[25] Previous studies have shown that miR-122-5p may be related to the polarization of macrophages,[26] at the same time, miR-122-5p also participates in inflammatory response by targeting TAK1,[27] and plays an important role in the body's inflammatory response. Microarray analysis has identified miR-122-5p in serum-derived exosomes,[28,29] and miR-122-5p is one of the miRNAs with the highest content in serum exosomes. However, the precise mechanism by which serum exosome miR-122-5p may impact liver and kidney injury in sepsis remains to be elucidated, and no relevant research findings have been obtained thus far.

LPS, a prevalent irritant in sepsis, has been employed as a model to simulate the inflammatory pathophysiology associated with sepsis-induced liver and kidney damage. In this study, an animal model of sepsis was established using LPS. Prior to modeling, some rats were treated with miR-122-5p inhibitor, exosome inhibitor (GW4869), and combined inhibitor. Afterward, exosomes were isolated from the animals' serum. The aim was to assess liver and kidney injury by measuring pro-inflammatory cytokine levels, indicators of organ damage, and NF-κB expression in liver and kidney tissues. Furthermore, the effects of miR-122-5p intervention and exosome production on these outcomes were evaluated to confirm the hypothesis that serum exosome miR-122-5p may cause liver and kidney injury through TAK1 up-regulation, SIRT1 down-regulation, ultimately leading to NF-kB activation. This could provide a scientific foundation for identifying new therapeutic targets for managing sepsis.

Materials and Methods

Animals

The find out about protocol was approved by the Ethics Committee of Lanzhou University Second Hospital. Wistar male rats weighing an average of 200 ± 20 g were obtained from the Animal Experimental Research Centre of Lanzhou University. All procedures pertaining to the handling of animals were conducted in accordance with the guidelines set forth in the Guide for the Care and Use of Laboratory Animals. All animal experimental procedures and protocols were approved by the Experimental Animal Welfare Ethics Committee of Lanzhou University Second Hospital (ethics number: D2024-012).

Patients

The study population consisted of sepsis patients admitted to the Department of Intensive Care Medicine at the Second Hospital of Lanzhou University from 1 January 2024 onwards, who met the diagnostic criteria for Sepsis 3.0. Non-sepsis patients were selected as the control group. After obtaining informed consent from either the patient or their family members, blood samples were collected to isolate serum exosomes. Non-sepsis patients were chosen as controls. Our

study complies with the Declaration of Helsinki. All clinical testing methods and protocols were approved by the Medical Ethics Committee of Lanzhou University Second Hospital (ethics number: 2024A-047).

Drugs, Kits, and Antibodies

LPS was purchased from Solarbio (China), and GW4869 was purchased form KKL Med (China). miR-122-5p inhibitor (miR-122-5p IN) and negative control (miR-122-5p NC) both constructed by Gemma Shanghai (China). All antibodies were purchased from Proteintech (China), and all ELISA kits were purchased from mlbio (China). All additional reagents are obtained from trusted suppliers.

LPS-Treated Rats and Pretreated with miR122-5p Inhibitor and GW4869 in the LPS-Rat Model

LPS endotoxemia model: LPS derived from *Escherichia coli* (Solarbio, China) was injected into male mice. Rats were randomly divided into seven groups: Control, LPS, miR122-5p inhibitor+LPS, miR122-5p NC+LPS, GW4869+LPS, GW4869, miR122-5p inhibitor+ GW4869+LPS.

Rats were pre-injected with PBS, GW4869, miR122-5p inhibitor, miR122-5p NC and miR122-5p inhibitor+ GW4869, respectively 2h before intraperitoneal injection of LPS to establish the PBS+LPS group, miR122-5p inhibitor+LPS, miR122-5p NC+LPS, GW4869+LPS group, miR122-5p inhibitor+ GW4869+LPS. The GW4869 crew used to be solely injected intraperitoneally with the exosome inhibitor GW4869 and the LPS team was once solely injected LPS, whilst the Control team obtained the identical quantity of PBS injection. The animals were euthanized 24h later using a high-dose intraperitoneal injection of pentobarbital (1%, mg/kg), and blood, liver and kidney tissues were collected immediately.

Exosome Isolation and Characterization

The rat blood samples were collected by centrifugation at 3,000 × g for 15 min at 4°C after being left at room temperature for two hours. The supernatant was then taken to obtain the serum, which was stored at −20°C or −80°C. Exosomes were isolated using differential centrifugation (all procedures performed at 4°C). Initially, equal volumes of serum samples were centrifuged at 2,000 × g for five min at 4°C. The resulting supernatant was transferred to a new tube and further centrifuged at 3,500 × g for 15–20 min. Subsequently, the supernatant was transferred to an ultra-high-speed centrifuge tube and subjected to centrifugation at 120,000 × g for one hundred twenty min in a Beckman ultracentrifuge (BECKMAN Optima L-100 XP). After discarding the supernatant, the pellet was resuspended in a solution of 1× phosphate buffer (PBS) and filtered through a 0.22 μm filter; the filtrate was collected and subjected to another round of centrifugation at 120,000 × g for one hundred twenty min. Again, the supernatant was discarded and the pellet resuspended in a solution of 1× PBS. For morphological transmission electron microscopy (TEM) analysis, exosome samples (10 μL) were dropped onto a copper grid and allowed to stand for three minutes before excess liquid was removed from the edges with filter paper. Then they were negatively stained with phosphotungstic acid (1%,10 μL) for five minutes followed by gentle aspiration of excess liquid with filter paper before placing them under a transmission electron microscope (HT7800, Japan) for observation and photography purposes. Exosomal protein quantification utilized dicinchoninic acid (BCA) assay kit(Biosharp, China), while Western blot analysis assessed expression levels of exosomal markers CD9, CD63, and CD81.

Total RNA Extraction, cDNA Synthesis, and Quantitative Real-Time Polymerase Chain Reaction (qRT-PCR)

The total RNA was extracted from the tissues using a rapid-pure RNA kit (AG RNAex Rro Reagent, China) according to the manufacturer's instructions. The integrity of RNA was assessed on 1% agarose gels, and the concentration and purity were determined using the Nano-Drop 2000 spectrophotometer (DENOVIX DS-11). Subsequently, cDNA synthesis was performed using the PrimeScript ™ RT reagent Kit (AG11705, ACCURATE BIOTECHNOLOGY, HUNAN) following the manufacturer's protocol. The cDNA templates were stored at −80°C until further analysis. The qRT-PCR assay was

conducted on a Rotor-Gene Q instrument (QIAGEN Rotor-Gene Q) with SYBR Premix Ex TaqTM (AG11701, ACCURATE BIOTECHNOLOGY, HUNAN). Each reaction mixture had a total volume of 20 μL containing two μL of diluted cDNA template (10-fold dilution in ddH2O), 10 μL SYBR Premix Ex TaqTM (AG11701, ACCURATE BIOTECHNOLOGY, HUNAN), 0.8 μL each of forward and reverse primers (10 mM), and 6.4 μL of ddH2O. The real-time PCR program consisted of an initial denaturation step at 95°C for 30s followed by forty cycles at 95°C for five s and then annealing/extension at 60°C for 30s. Melting curve analysis was performed after amplification to ensure product homogeneity across all reactions while non-template reactions served as negative controls showing no amplification signal when water instead of cDNA was used as template DNA source. Amplification efficiencies were calculated based on standard curves generated from serial dilutions (1:10) of cDNA samples. The primer sequences used were as follows: miR122-5p: forward - CGGCTGGAGTGTGACAATGG −3′; reverse - ACTGCAGGGTCCGAGGTATT-3′; U6 primer: forward - GGAACGATACAGAGAAGATTAGC-3′; reverse - GGAACGATACAGAGA AGATT AGC −3′. All qRT-PCRs were performed in triplicate with repeated assays. The mRNA levels of each target gene were quantified using the real-time PCR Ct (2–ΔΔCT) relative quantitative method, with U6 as the reference gene for normalization.

Elisa

Rat serum was collected 24 hours post-surgery, and the levels of tumor necrosis factor-α (TNF-α), interleukin-6 (IL-6), lactate dehydrogenase (LDH), and interleukin-1β (IL-1β) in the serum were quantified using an enzyme-linked immunosorbent assay (ELISA) kit from Mlbio, China, following the manufacturer's instructions.

Serum Indicators of Liver and Kidney Injury

The serum levels of aspartate aminotransferase (AST), alanine aminotransferase (ALT), urea, creatinine, and uric acid (UA) in each group were quantified using computerized biochemical analysis.

Histopathology/H&E Staining

The liver or kidney tissues of rats were fixed in 4% paraformaldehyde for 24 hours, dehydrated using an alcohol gradient, embedded in paraffin, and then prepared as 4 μm tissue sections. These sections were stained with a hematoxylin eosin (H&E) staining kit (Beyotime, China), observed and photographed using an optical microscope (TissueFAXS Plus). Histologic scoring was conducted on a scale of 0–5, with scoring parameters including interstitial edema, hemorrhage, and neutrophil infiltration.

Immunofluorescence

After dewaxing the paraffin sections, antigen retrieval was performed. Endogenous peroxidase activity was blocked and serum was incubated at room temperature for 30 minutes. The primary antibody was then incubated overnight at 4°C. Subsequently, the secondary antibody was incubated at room temperature for 50 minutes. After washing, the slices were gently dried and a freshly prepared DAB color development solution was added to each section. The color development time was carefully controlled under a microscope. A desirable brown and yellow coloration indicated successful staining, followed by termination of the reaction with tap water washes. Hematoxylin counterstaining of nuclei lasted approximately three minutes before rinsing with tap water. Sequential dehydration steps included immersion in 75% alcohol for five minutes, followed by 85% alcohol for another five minutes, anhydrous ethanol I and II each for five minutes respectively, n-butanol for five minutes, and xylene for five more minutes until transparency achieved. Finally, the sections were air-dried after removal from xylene and sealed with adhesive glue prior to imaging using an optical microscope (TissueFAXS Plus).

Western Blotting (WB)

The liver and kidney tissues were homogenized using a tissue homogenizer. Subsequently, the exosomes and liver and kidney tissue homogenates were lysed with RIPA cleavage buffer containing a protease inhibitor mixture (Solarbio, China). Total protein quantification was performed using a BCA kit (Biosharp, China), followed by denaturation through boiling. Equal amounts of protein were loaded onto an SDS-PAGE gel for electrophoretic separation. The separated

proteins were then transferred to a polyvinylidene fluoride (PVDF) membrane and sealed with 5% skim milk solution at room temperature for 2 hours. Next, incubation with Proteintech antibodies (China) was carried out overnight at 4°C. Afterward, the membranes were incubated with secondary antibodies (Proteintech, China; diluted 1:2000) at room temperature for 1 hour before being developed using a hypersensitive ECL chemiluminescence kit (NCM Biotech, China). Finally, detection was performed using a multifunctional imaging system (T Tanon 5200 Multi, China).

Statistical Analysis

The statistical data were analyzed using GraphPad Prism eight software and SPSS 20.0. Measurements were expressed as mean ± standard deviation (SD). Kolmogorov–Smirnov tests were employed to assess the normal distribution of the data. For normally distributed data, a two-sample *t*-test was used for comparison between two groups, while analysis of variance (ANOVA) was utilized for comparison among multiple groups. Non-parametric Kruskal–Wallis test and Dunn's multiple comparison test were applied for non-normally distributed data, such as histological results. A p-value less than 0.05 was considered statistically significant. Data from in vivoexperiments were presented as mean ± standard error of the mean (SEM), and one-way analysis of variance (ANOVA) followed by Tukey's test was performed for multiple comparisons. All procedures were repeated three times with a significance level set at $p < 0.05$.

Results

LPS Modeling in Rats

In comparison to the control group, the LPS group exhibited numerous punctate necrotic lesions on the liver surface, along with observed kidney hyperemia and swelling due to LPS administration. Histopathological examination using HE staining revealed that the control group displayed normal liver tissue structure with orderly cell arrangement and absence of pathological phenomena. Conversely, the model group exhibited evident liver tissue lesions characterized by edema, degeneration, and necrosis of hepatocytes, as well as infiltration of inflammatory cells. The kidneys in the control group showed intact structure without bleeding or inflammatory infiltration; however, in the LPS group, tubular epithelial cells demonstrated edema with increased cell volume, disordered glomerular structure, narrowed tubular lumen, significant bleeding within interstitium accompanied by a large number of infiltrating inflammatory cells. Treatment with miR-122-5p inhibitor+LPS or GW4869+LPS or miR122-5p inhibitor+GW4869+LPS effectively alleviated inflammation and improved acute organ injury in septic mice.

Characterization and Analysis of Exosomes

We isolated exosomes from rat serum using ultrafast centrifugation and characterized their size and concentration through particle size analysis. The majority of particles (over 80%) had a diameter ranging from 30 to 120 nm, with an average size of 101 nm, consistent with the typical size range of exosomes. Additionally, intact cup-shaped membrane vesicles were observed under transmission electron microscopy (TEM), and the expression levels of three common exosome markers - CD9, CD63, and CD81 - were confirmed by Western blotting (Figure 1).

The Content of miR-122-5p in Exosomes and Liver and Kidney Tissues Was Determined by PCR

The PCR results revealed that the expression of miR-122-5p in serum exosomes was significantly elevated in septic patients compared to non-septic individuals, and there was a marked increase in the levels of miR-122-5p observed in serum exosomes, liver tissues, and kidney tissues of septic rats when compared to controls ($p<0.05$) (Figure 2).

Circulating Pro-Inflammatory Cytokines

The levels of pro-inflammatory cytokines (TNF-α, IL-1β, LDH, and IL-6) in the serum of LPS-treated rats were significantly elevated. In contrast, pretreatment with GW4869, a miR122-5p inhibitor, or their combination markedly attenuated the production of pro-inflammatory cytokines in response to endotoxin stimulation. (The levels of serum inflammatory factors in each group were compared in the Supplementary Tables 1–4).

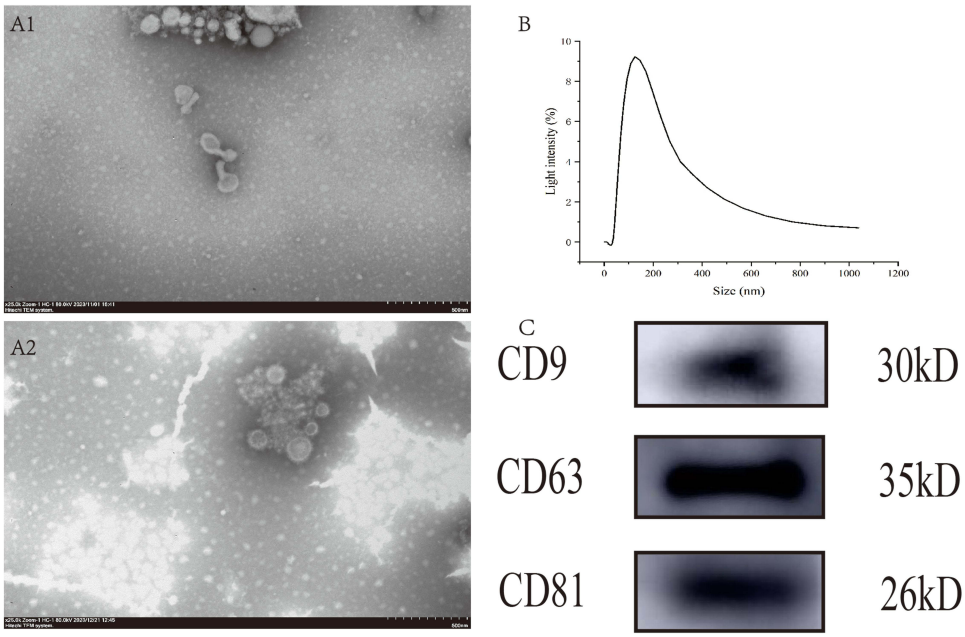

Figure 1 Results of serum exosome identification (**A**) morphology of Serum-EXOs under transmission electron microscopy. Exosomes photographed by electron microscopy at two angles are shown in Figure A1-A2. All size bar is 500 nm. (**B**) Range of concentration of ion diameter of Serum-EXOs detected by zeta potential particle size analyzer; (**C**) Detection of the surface marker proteins of CD9, CD63, and CD81 on Serum-Exos by Western blot.

Liver and Kidney Function

After 24 hours of modeling, tissue samples were collected and subjected to constant and HE staining. The morphological changes in the kidney were observed using light microscopy. Histomorphological alterations in the liver were examined under a light microscope. The hepatocyte morphology in the control and GW4869 groups appeared normal and well-organized. In the LPS group, disruption of liver lobule structure, hepatocyte swelling and necrosis, as well as infiltration of inflammatory cells were observed. However, compared to the LPS group, these liver pathological changes were partially alleviated in the miR-122-5p inhibitor+LPS, GW4869+LPS, and miR-122-5p inhibitor+GW4869+LPS groups. Regarding renal function index changes, serum AST and ALT levels significantly increased in rats from the LPS group. Conversely, serum AST and ALT levels significantly decreased in the miR-122-5p inhibitor+LPS, GW4869+LPS, and miR-122-5p inhibitor+GW4869+LPS groups when compared with the LPS group ($P<0.05$).

The renal morphology of the control and GW4869 groups remained intact, with no evidence of inflammatory cell infiltration or tissue edema in the renal tissue. In contrast, the LPS group exhibited blurred renal morphology, evident tissue edema, and increased inflammatory cell infiltration. This was accompanied by glomerular deformation and enlargement, as well as dilatation of renal tubules. Epithelial cell swelling, brush border detachment, and apparent vacuolar degeneration were also observed along with sporadic bleeding.

The pathological changes in glomeruli, renal interstitium, and renal tubules were significantly reduced in the miR122-5p inhibitor+LPS group, GW4869+LPS group, and miR122-5p inhibitor+GW4869+LPS group compared to the LPS group. Furthermore, alterations in serum UREA (urea nitrogen), CREA (creatinine), UA (uric acid), AST (aspartate aminotransferase), and ALT (alanine aminotransferase) levels were consistent with these histological findings ($P < 0.05$) (Figure 3).

Immunohistochemistry

Compared to the control group, the expression level of TAK1 was upregulated in liver and kidney tissues of rats in the LPS group. However, co-administration of miR-122-5p inhibitor with LPS, GW4869 with LPS, or miR-122-5p inhibitor with GW4869 and LPS effectively attenuated the upregulation of TAK1 expression in liver and kidney tissues. SIRT1 expression levels were downregulated in liver and kidney tissues of the LPS group. Nevertheless, co-treatment with

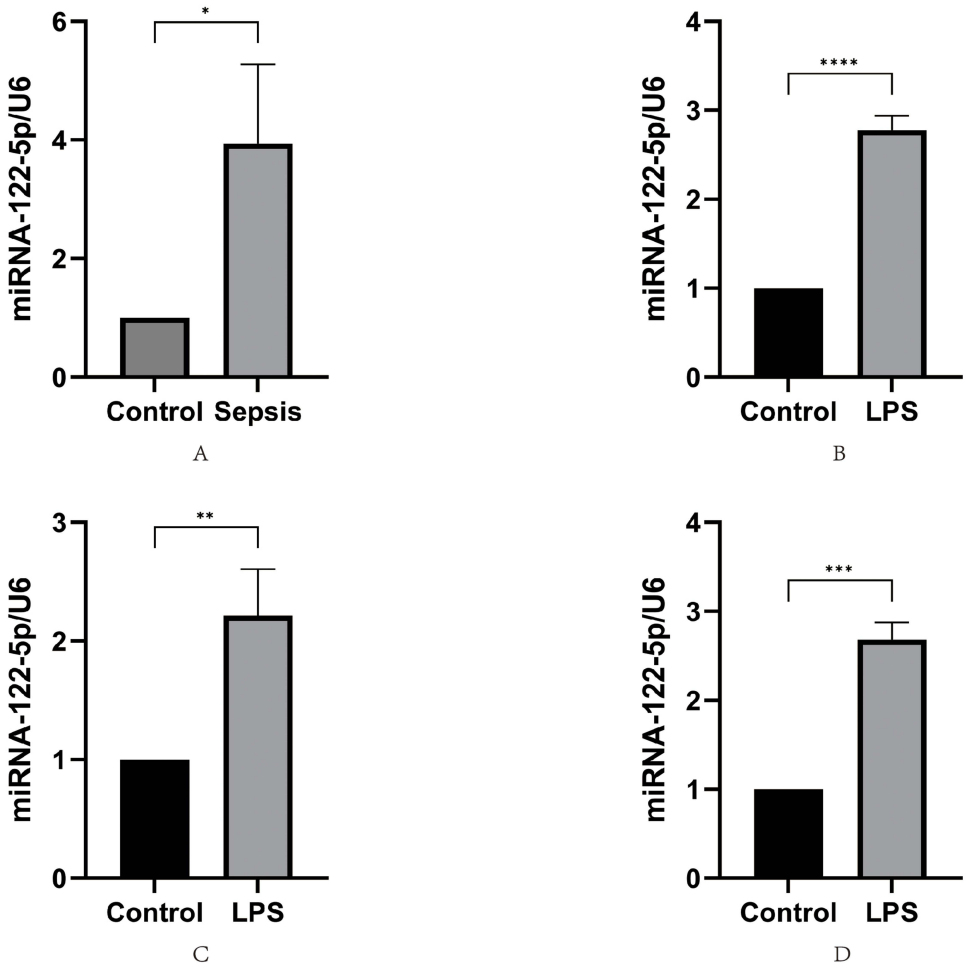

Figure 2 The results of the PCR demonstrated notable discrepancies. (**A**) Comparison of miR-122-5p levels in serum exosomes between septic and non-septic patients. (**B**) Comparison of miR-122-5p levels in serum exosomes between LPS-induced rats and control rats. (**C**) Comparison of miR-122-5p levels in liver tissues between LPS-induced rats and control rats. (**D**) Comparison of miR-122-5p levels in kidney tissues between LPS-induced rats and control rats. The data are presented as means ± standard error (n=3). All data are expressed as mean ± standard deviation. *P < 0.05; **P < 0.01, ***P < 0.001, ****P < 0.0001, compared to the control group.

miR122-5p inhibitor and LPS, GW4869 and LPS, or miR122-5p inhibitor with GW4869 and LPS significantly enhanced SIRT1 expression in liver and kidney tissues (compared to both control group and LPS group) (Figure 4).

Serum Exosome Activates NF-κB Signaling Pathway in Liver and Kidney Tissues via miR-122-5p

Compared to the control group, the LPS group exhibited upregulated expression of NF-κB pp65 protein in both liver and kidney of rats. However, treatment with miR122-5p inhibitor+LPS, GW4869+LPS, or miR122-5p inhibitor+GW4869 +LPS effectively attenuated this upregulation of NF-κB pp65 protein expression in both liver and kidney (compared to the control and LPS groups) (Figure 5).

Discussion

Given its high mortality rate, sepsis poses a significant global health challenge and imposes substantial economic burdens. The grave implications of sepsis necessitate the development of more efficacious treatment strategies to enhance clinical outcomes.[30] The intricate pathophysiology of sepsis, characterized by multi-organ dysfunction, has impeded the development of efficacious therapeutic drugs for its treatment. Among sepsis patients, the most prevalent organ failures occur in the kidney (56.9%), cardiovascular system (24.3%), central nervous system (20.7%), respiratory system

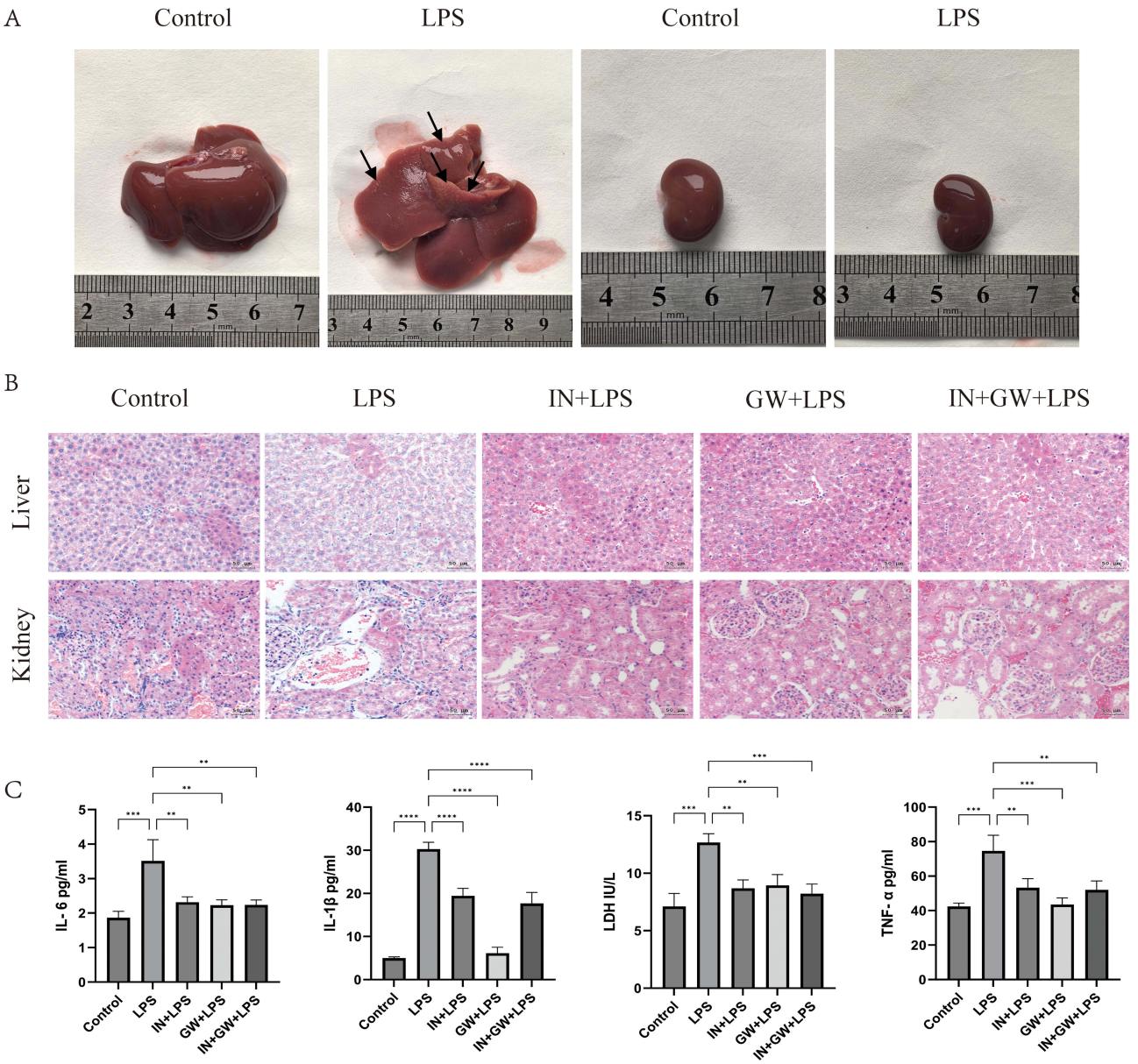

Figure 3 Significant differences were observed in the levels of liver and kidney injury and inflammation among all groups. (**A**) Comparison of liver and kidney morphology between the control and LPS groups revealed distinct differences. The LPS group exhibited evident punctate necrotic foci on the surface of the liver (Necrotic lesions on the liver surface are indicated by the black arrow), while congestion was observed in the kidneys. (**B**) H&E staining analysis demonstrated that pathological alterations in the liver and kidneys were partially ameliorated in miR-122-5p IN+LPS, GW+LPS, and miR-122-5p IN+GW+LPS groups compared to the LPS group. All size bar is 50 μm. (**C**) Inhibitor treatment significantly reduced serum levels of tumor necrosis factor-alpha (TNF-α), interleukin-6 (IL-6), lactate dehydrogenase (LDH), and interleukin-1 beta (IL-1β) compared to those in the LPS group. Data are presented as means ± SE (n=3). All data are mean ± SD. **P < 0.01, ***P < 0.001, ****P < 0.0001, compared with control group.

(15.2%), and blood system (10.3%). Notably, sepsis patients are particularly susceptible to kidney impairment, with acute kidney injury (AKI) frequently observed at disease onset or during treatment. A 2019 study examining over 20,000 sepsis patients using 29 early clinical indicators identified four distinct phenotypes: alpha, beta, gamma, and delta; among these phenotypes, delta exhibited the highest mortality rate and a heightened propensity for liver dysfunction and shock.[31] The liver is seen as the "guardian, regulator, and target" of sepsis and is central to immune regulation in response to systemic infections[32]. Consistent with the results of this study, reduced ALT, AST and TNF-α levels are considered biomarkers of protective effects in LPS-induced animal models.[33] It has also been found that injecting exosomes produced by LPS-stimulated macrophages into mice causes damage to kidney endothelial cells.[34] The serum levels of UREA, CREA, and

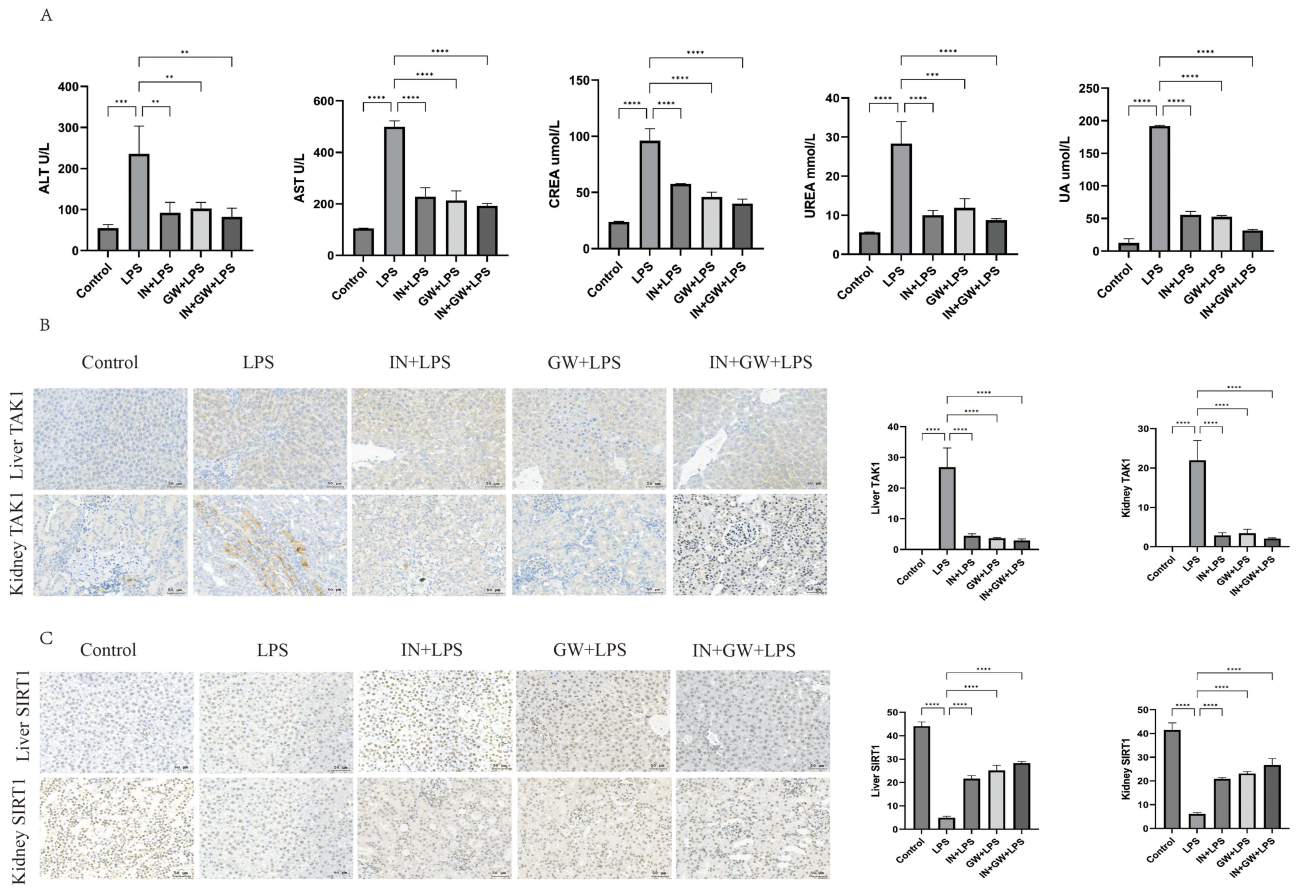

Figure 4 The expression level of the upstream protein was determined through immunohistochemical analysis. (**A**) The serum levels of aspartate aminotransferase (AST), alanine aminotransferase (ALT), urea, creatinine, and uric acid in rats were measured in each experimental group. (**B** and **C**) Immunohistochemical analysis was performed to compare the expression of TAK1 and SIRT1 in the liver and kidney tissues of rats from each group. Statistical significance was determined using one-way ANOVA followed by Tukey's post hoc test, revealing significant differences between LPS-treated group vs control group ($p < 0.05$), IN+LPS-treated group vs LPS-treated group ($p < 0.05$), GW +LPS-treated group vs LPS-treated group, and IN +GW+LPS-treated group vs LPS-treated group ($p < 0.05$). **P < 0.01, ***P < 0.001, ****P < 0.0001, compared with control group. All size bar is 50 μm.

UA in rats from the miR-122-5p inhibitor+LPS, GW4869+LPS, and miR-122-5p inhibitor+GW4869+LPS groups were significantly lower compared to those in the LPS group. These findings suggest that exosome-derived miR-122-5p can induce kidney damage while miR-122-5p inhibitors can alleviate sepsis-induced kidney injury. Furthermore, pretreatment not only attenuated the elevation of liver and kidney injury markers caused by LPS stimulation but also reduced serum inflammatory cytokine levels and NF-kB signaling pathway activation in liver and kidney tissues, ultimately mitigating sepsis-induced liver and kidney injury. Although this study primarily focused on liver and kidney tissue, other studies have demonstrated a strong association between exosomes and sepsis-related cardiopulmonary damage.[35,36]

The exosomes derived from sepsis also alleviate the condition by inducing macrophage polarization, characterized by a significant shift from the pro-inflammatory M1 phenotype to the anti-inflammatory M2 phenotype.[37–39] Previous studies have shown that miR-122-5p may be related to the polarization of macrophages,[26] and some other studies have found: Interleukin-1β (IL-1β) pretreated mouse mesenchymal stem cell (MSCs) exosomes can effectively induce M2-like polarization of macrophages in vitro and in vivo, reducing TNF-α, interleukin-6 (IL-6), and interleukin-1β (IL-1β).[40] Other studies have shown that exosomes can worsen the disease:[41,42] In sepsis associated acute lung injury, exosomes induce M1 macrophage polarization and macrophage pyrodeath by activating NF-κB. Some studies have found that exosomes induce M1 macrophage polarization and induce macrophage pyroptosis by activating NF-κB in sepsis related acute lung injury.[43] Based on these findings, our team hypothesized that the presence of miR-122-5p in exosomes is closely associated with macrophage proliferative polarization during the onset and progression of sepsis. Moving

https://doi.org/10.2147/IDR.S499643

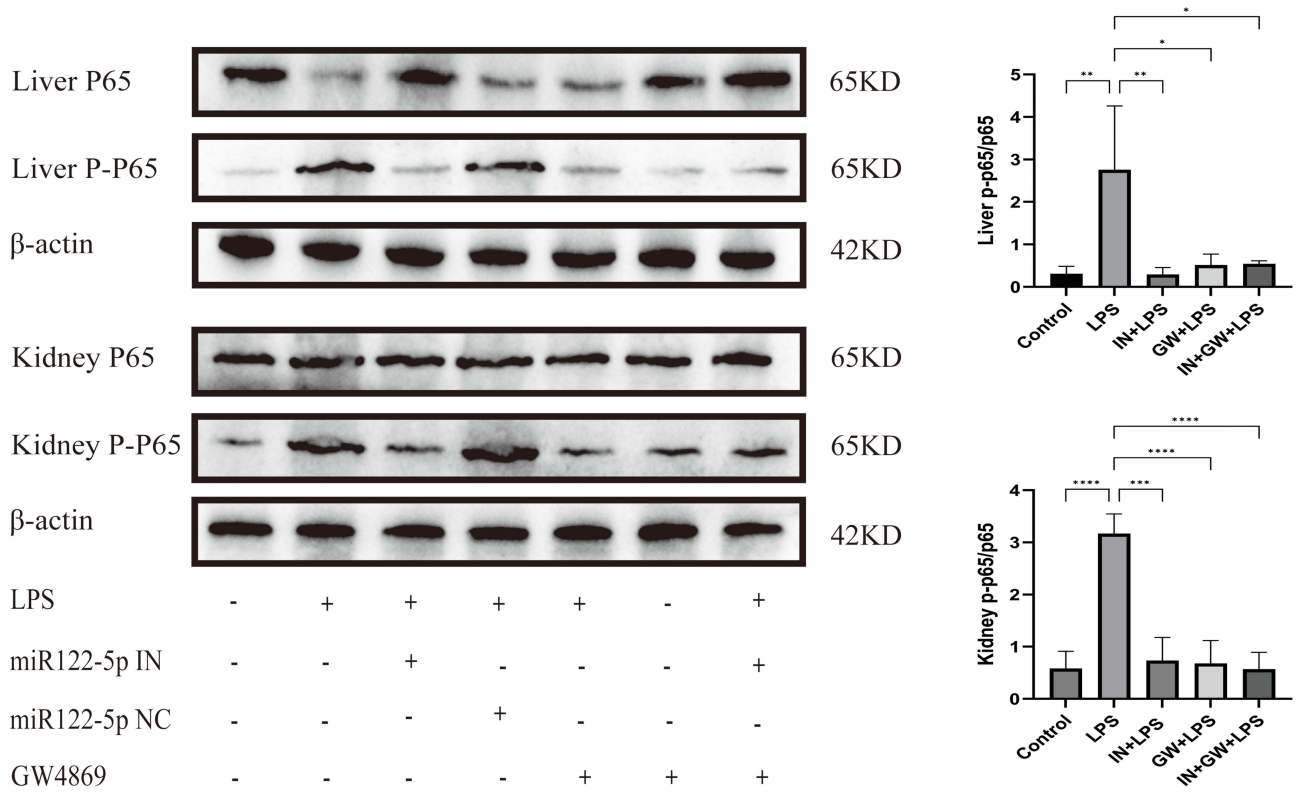

Figure 5 The activation of the NF-κB pathway was confirmed through Western blot analysis. Expression of P65 and P-P65 protein was determined by Western blot analysis. Data are represented as means ± SE (n=3). Multiple comparisons by one-way ANOVA and Tukey's-post hoc showed statistical significance at: LPS vs control group ($p < 0.05$), IN+LPS vs LPS group ($p < 0.05$), GW+LPS vs LPS and IN +GW+LPS vs LPS group ($p < 0.05$). * $P < 0.05$; ** $P < 0.01$, *** $P < 0.001$, **** $P < 0.0001$, compared with control group.

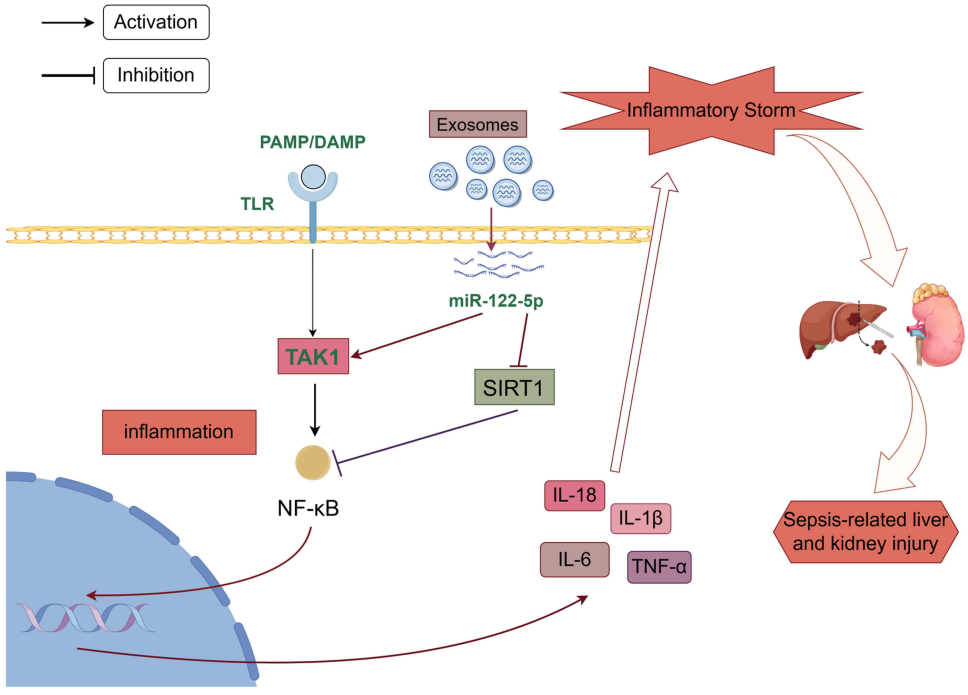

Figure 6 Mechanism of exosomal miR-122-5p regulation of hepatic and renal injury in sepsis. Serum exosome miR-122-5p can promote the levels of serum inflammatory factors and liver and kidney injury indices in rats induced by LPS, up-regulate TAK1, down-regulate SIRT1, and ultimately promote the activation of NF-κB, leading to liver and kidney injury. (By Figdraw.).

https://doi.org/10.2147/IDR.S499643

forward, our team will focus on investigating the correlation between serum exosome levels and macrophage proliferative polarization in sepsis. In our study, we observed that serum exosomal miR-122-5p can impact the NF-κB pathway; however, specific effects were not included in the experimental content. Therefore, we utilized big data analysis to screen potential targets of miR-122-5p and identified a total of 5 genes which were further analyzed through co-expression pathways to explore possible downstream targets. This approach provides a foundation for future studies examining the relationship between serum exosomal miR-122-5p and the NF-κB pathway (Supplementary Figure 1).

However, there are several limitations in this study that need to be addressed. Firstly, the use of only one modelling method (LPS stimulation) to simulate rat sepsis may not fully capture the complexity of the disease. Secondly, a quantitative standard for assessing the progression of sepsis patients was lacking, which could have affected the accuracy and reliability of the results. Additionally, the absence of concentration gradient administration limited our understanding of dose-dependent effects. Future studies should consider incorporating both LPS and CLP models simultaneously to enhance their validity and explore multi-group drug concentration gradients for comprehensive analysis. The objective of this study was to investigate the potential of miR-122-5p inclusion in serum exosomes for mitigating sepsis-induced liver and kidney damage. Based on the experimental data, it was observed that elevated levels of serum exosome miR-122-5p were closely associated with sepsis-induced liver and kidney damage as well as systemic inflammation. Furthermore, it was discovered that serum exosome miR-122-5p upregulated TAK1, downregulated SIRT1, ultimately leading to NF-κB activation and subsequent liver and kidney injury. These findings offer promising therapeutic strategies for addressing severe inflammatory storms and organ dysfunction in sepsis at a cellular level.

Conclusion

Based on our findings, it can be inferred that the regulatory effects of Serum exosomes miR-122-5P play a pivotal role in sepsis-induced liver and kidney injury. The utilization of miR122-5p and GW4869 inhibitors mitigates hepatic and renal injury by modulating serum hepatic and renal injury indexes, inhibiting TAK1 activation, promoting SIRT1 expression, and ultimately suppressing pathway activation to attenuate hepatic and renal injury. Consequently, Serum exosome miR-122-5p facilitates the elevation of serum inflammatory factors as well as liver and kidney injury indices in LPS-induced rats, upregulates TAK1 expression while downregulating SIRT1 levels, thereby facilitating NF-κB activation leading to liver and kidney injury (Figure 6).

Acknowledgments

We would like exhibit honest perception to the reviewers for essential remarks regarding this article. We appreciate the Figdraw website for its help in drawing Figure 6.

Author Contributions

Li Ma provided research direction and support. Jiaqi Wang wrote the manuscript. All authors made a significant contribution to the work reported, whether that is in the conception, study design, execution, acquisition of data, analysis and interpretation, or in all these areas; took part in drafting, revising or critically reviewing the article; gave final approval of the version to be published; have agreed on the journal to which the article has been submitted; and agree to be accountable for all aspects of the work.

Funding

This study was supported by the Natural Science Foundation of Gansu Province (No.22JR5RA965).

Disclosure

The authors report no conflicts of interest in this work.

References

1. Rudd KE, Johnson SC, Agesa KM, et al. Global, regional, and national sepsis incidence and mortality, 1990-2017: analysis for the global burden of disease study. *Lancet*. 2020;395:200–211. doi:10.1016/S0140-6736(19)32989-7

2. Prescott HC, Angus DC. Enhancing recovery from sepsis: a review. *JAMA*. 2018;319:62–75. doi:10.1001/jama.2017.17687
3. Ogawa Y, Taketomi Y, Murakami M, Tsujimoto M, Yanoshita R. Small RNA transcriptomes of two types of exosomes in human whole saliva determined by next generation sequencing. *Biol Pharm Bull*. 2013;36:66–75. doi:10.1248/bpb.b12-00607
4. Torregrosa Paredes P, Gutzeit C, Johansson S, et al. Differences in exosome populations in human breast milk in relation to allergic sensitization and lifestyle. *Allergy*. 2014;69:463–471. doi:10.1111/all.12357
5. Kesimer M, Scull M, Brighton B, et al. Characterization of exosome-like vesicles released from human tracheobronchial ciliated epithelium: a possible role in innate defense. *FASEB J*. 2009;23:1858–1868. doi:10.1096/fj.08-119131
6. Shao H, Im H, Castro CM, et al. New technologies for analysis of extracellular vesicles. *Chem Rev*. 2018;118:1917–1950. doi:10.1021/acs.chemrev.7b00534
7. Zhang Y, Liu Y, Liu H, Tang WH. Exosomes: biogenesis, biologic function and clinical potential. *Cell Biosci*. 2019;9:19. doi:10.1186/s13578-019-0282-2
8. Gui Y, Liu H, Zhang L, Lv W, Hu X. Altered microRNA profiles in cerebrospinal fluid exosome in Parkinson disease and Alzheimer disease. *Oncotarget*. 2015;6:37043–37053. doi:10.18632/oncotarget.6158
9. Kalluri R, LeBleu VS. The biology, function, and biomedical applications of exosomes. *Science*. 2020;367. doi:10.1126/science.aau6977
10. Zheng X, Chen F, Zhang Q, et al. Salivary exosomal PSMA7: a promising biomarker of inflammatory bowel disease. *Protein and Cell*. 2017;8:686–695. doi:10.1007/s13238-017-0413-7
11. Szul T, Bratcher PE, Fraser KB, et al. Toll-like receptor 4 engagement mediates prolyl endopeptidase release from airway epithelia via exosomes. *Am J Respir Cell Mol Biol*. 2016;54:359–369. doi:10.1165/rcmb.2015-0108OC
12. Li ZG, Scott MJ, Brzóska T, et al. Lung epithelial cell-derived IL-25 negatively regulates LPS-induced exosome release from macrophages. *Mil Med Res*. 2018;5:24. doi:10.1186/s40779-018-0173-6
13. Yang C, Robbins PD. The roles of tumor-derived exosomes in cancer pathogenesis. *Clin Dev Immunol*. 2011;2011:842849. doi:10.1155/2011/842849
14. Delic D, Eisele C, Schmid R, et al. Urinary exosomal miRNA signature in type II diabetic nephropathy patients. *PLoS One*. 2016;11:e0150154. doi:10.1371/journal.pone.0150154
15. Santucci L, Bruschi M, Candiano G, et al. Urine proteome biomarkers in kidney diseases. I. Limits, perspectives, and first focus on normal urine. *Biomark Insights*. 2016;11:41–48. doi:10.4137/BMI.S26229
16. Mooberry MJ, Bradford R, Hobl EL, et al. Procoagulant microparticles promote coagulation in a factor XI-dependent manner in human endotoxemia. *J Thromb Haemost*. 2016;14:1031–1042. doi:10.1111/jth.13285
17. Janiszewski M, Do Carmo AO, Pedro MA, et al. Platelet-derived exosomes of septic individuals possess proapoptotic NAD(P)H oxidase activity: a novel vascular redox pathway. *Crit Care Med*. 2004;32:818–825. doi:10.1097/01.ccm.0000114829.17746.19
18. Li L, Huang L, Huang C, et al. The multiomics landscape of serum exosomes during the development of sepsis. *J Adv Res*. 2022;39:203–223. doi:10.1016/j.jare.2021.11.005
19. Wang X, Huang J, Chen W, et al. The updated role of exosomal proteins in the diagnosis, prognosis, and treatment of cancer. *Exp Mol Med*. 2022;54:1390–1400. doi:10.1038/s12276-022-00855-4
20. Krol J, Loedige I, Filipowicz W. The widespread regulation of microRNA biogenesis, function and decay. *Nat Rev Genet*. 2010;11:597–610. doi:10.1038/nrg2843
21. Condorelli G, Latronico MV, Cavarretta E. microRNAs in cardiovascular diseases: current knowledge and the road ahead. *J Am Coll Cardiol*. 2014;63:2177–2187. doi:10.1016/j.jacc.2014.01.050
22. Wronska A, Kurkowska-Jastrzebska I, Santulli G. Application of microRNAs in diagnosis and treatment of cardiovascular disease. *Acta Physiol*. 2015;213:60–83. doi:10.1111/apha.12416
23. Shi MM, Zhu Y-G, Yan J-Y, et al. Role of miR-466 in mesenchymal stromal cell derived extracellular vesicles treating inoculation pneumonia caused by multidrug-resistant Pseudomonas aeruginosa. *Clin Transl Med*. 2021;11:e287. doi:10.1002/ctm2.287
24. El Gazzar M, McCall CE. MicroRNAs distinguish translational from transcriptional silencing during endotoxin tolerance. *J Biol Chem*. 2010;285:20940–20951. doi:10.1074/jbc.M110.115063
25. Real JM, Ferreira LRP, Esteves GH, et al. Exosomes from patients with septic shock convey miRNAs related to inflammation and cell cycle regulation: new signaling pathways in sepsis? *Critical Care*. 2018;22:68. doi:10.1186/s13054-018-2003-3
26. Zhao Z, Zhong L, Li P, et al. Cholesterol impairs hepatocyte lysosomal function causing M1 polarization of macrophages via exosomal miR-122-5p. *Exp Cell Res*. 2020;387:111738. doi:10.1016/j.yexcr.2019.111738
27. Zheng W, Chang R, Luo Q, Liu G, Xu T. The long noncoding RNA MIR122HG is a precursor for miR-122-5p and negatively regulates the TAK1-induced innate immune response in teleost fish. *J Biol Chem*. 2022;298:101773. doi:10.1016/j.jbc.2022.101773
28. Xu J, Feng Y, Jeyaram A, et al. Circulating plasma extracellular vesicles from septic mice induce inflammation via MicroRNA- and TLR7-dependent mechanisms. *J Immunol*. 2018;201:3392–3400. doi:10.4049/jimmunol.1801008
29. Li DB, Liu J-L, Wang W, et al. Plasma exosomal miRNA-122-5p and miR-300-3p as potential markers for transient ischaemic attack in rats. *Front Aging Neurosci*. 2018;10:24. doi:10.3389/fnagi.2018.00024
30. Gavelli F, Castello LM, Avanzi GC. Management of sepsis and septic shock in the emergency department. *Intern Emerg Med*. 2021;16:1649–1661. doi:10.1007/s11739-021-02735-7
31. Seymour CW, Kennedy JN, Wang S, et al. Derivation, validation, and potential treatment implications of novel clinical phenotypes for sepsis. *JAMA*. 2019;321:2003–2017. doi:10.1001/jama.2019.5791
32. Lelubre C, Vincent JL. Mechanisms and treatment of organ failure in sepsis. *Nat Rev Nephrol*. 2018;14:417–427. doi:10.1038/s41581-018-0005-7
33. Strnad P, Tacke F, Koch A, Trautwein C. Liver - guardian, modifier and target of sepsis. *Nat Rev Gastroenterol Hepatol*. 2017;14:55–66. doi:10.1038/nrgastro.2016.168
34. Xiang H, Xu Z, Zhang C, Xiong J. Macrophage-derived exosomes mediate glomerular endothelial cell dysfunction in sepsis-associated acute kidney injury. *Cell Biosci*. 2023;13:46. doi:10.1186/s13578-023-00990-z
35. Jiang K, Yang J, Guo S, et al. Peripheral circulating exosome-mediated delivery of miR-155 as a novel mechanism for acute lung inflammation. *Mol Ther*. 2019;27:1758–1771. doi:10.1016/j.ymthe.2019.07.003
36. Terrasini N, Lionetti V. Exosomes in critical illness. *Crit Care Med*. 2017;45:1054–1060. doi:10.1097/ccm.0000000000002328

37. Pan Y, Hui X, Hoo RLC, et al. Adipocyte-secreted exosomal microRNA-34a inhibits M2 macrophage polarization to promote obesity-induced adipose inflammation. *J Clin Invest*. 2019;129:834–849. doi:10.1172/jci123069
38. Shen K, Jia Y, Wang X, et al. Exosomes from adipose-derived stem cells alleviate the inflammation and oxidative stress via regulating Nrf2/HO-1 axis in macrophages. *Free Radic Biol Med*. 2021;165:54–66. doi:10.1016/j.freeradbiomed.2021.01.023
39. Fan L, Yao L, Li Z, et al. Exosome-based mitochondrial delivery of circRNA mSCAR alleviates sepsis by orchestrating macrophage activation. *Adv Sci*. 2023;10:e2205692. doi:10.1002/advs.202205692
40. Yao M, Cui B, Zhang W, et al. Exosomal miR-21 secreted by IL-1β-primed-mesenchymal stem cells induces macrophage M2 polarization and ameliorates sepsis. *Life Sci*. 2021;264:118658. doi:10.1016/j.lfs.2020.118658
41. O'Neill HC, Quah BJ. Exosomes secreted by bacterially infected macrophages are proinflammatory. *Sci Signaling*. 2008;1:pe8. doi:10.1126/stke.16pe8
42. Zhao J, Chen X-D, Yan -Z-Z, et al. Gut-derived exosomes induce liver injury after intestinal ischemia/reperfusion by promoting hepatic macrophage polarization. *Inflammation*. 2022;45:2325–2338. doi:10.1007/s10753-022-01695-0
43. Jiao Y, Zhang T, Zhang C, et al. Exosomal miR-30d-5p of neutrophils induces M1 macrophage polarization and primes macrophage pyroptosis in sepsis-related acute lung injury. *Critical Care*. 2021;25:356. doi:10.1186/s13054-021-03775-3